A study on the energy transfer of a square prism under fluid-elastic galloping

H.G.K.G. Jayatunga, B.T. Tan, J. S. Leontini

Abstract

Extracting useful energy from flow induced vibrations has become a developing area of research in recent years. In this paper, we analyse power transfer of an elastically mounted body under the influence of fluid-elastic galloping. The system and the power transfer is analysed by numerically integrating the quasi-steady state model equations and direct numerical simulations. The power transfer is analysed for both high ($Re = 22300$) and low ($Re = 200$) Reynolds numbers cases.

The linear analysis of the model equation shows that the system is governed by two parameters, namely the combined mass-stiffness parameter Π_1 and the combined mass damping parameter Π_2. A combined mass-damping coefficient, Π_2, that can be derived from the equation of motion, is shown to be the parameter that governs power output. The system is a balance between the power delivered to the system due to fluid-dynamic forcing and power removed through mechanical damping which are governed by the fluid-dynamic forcing characteristics (i.e. the lift force as a function of incident angle) and mechanical damping coefficient as represented by Π_2 respectively. Comparing the DNS results with the QSS data uncovered that a good agreement of the data could be obtained even at low Reynolds numbers when the mass-stiffness,Π_1, is high representing a high mass to stiffness ratio. At low Π_1, the system shows a significant response to forces associated with shedding and this is shown to suppress the galloping response.

Keywords:

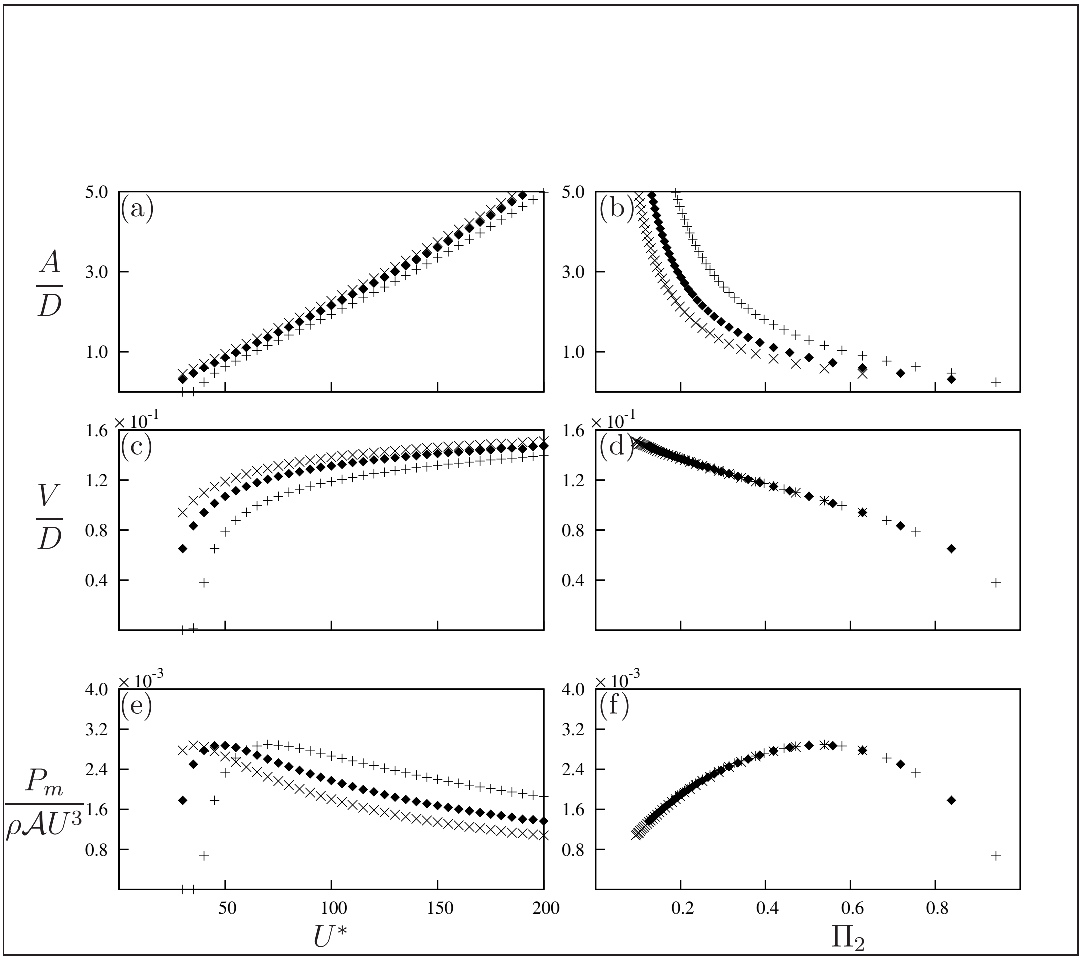

Figure 1: Displacement amplitude, velocity amplitude and mean power data as functions of two different independent varibles. Data presented in (a), (c) and (e) using the classical VIV parameter U^*, obtained at $Re = 200$ and $m^* = 20$ at three different damping ratios: $\zeta = 0.075$ ($\times$), $\zeta = 0.1$ (◆) and $\zeta = 0.15$ ($+$). (b) (d) and (f) are the same data presented using the combined mass-damping parameter (Π_2) as the independent variable.

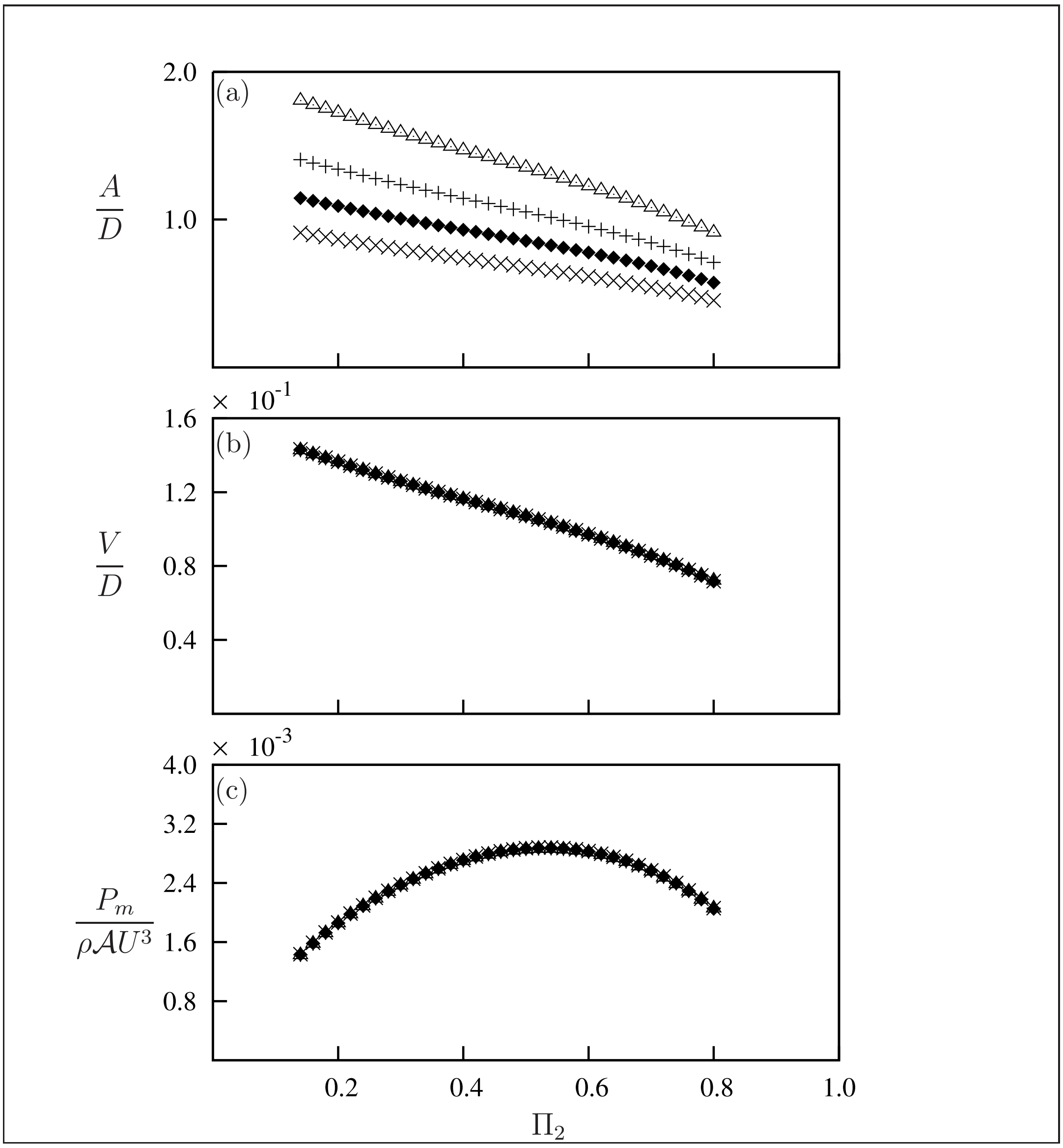

Figure 2: QSS data at high Π_1 levels. (a) displacement amplitude, (b) velocity amplitude and (c) mean power as a function of Π_2. Data presented at four different combined mass-stiffness levels. $\Pi_1 = 10$ ($m^* = 20,\ U^* = 40$) ($\times$), $\Pi_1 = 100$ ($m^* = 80,\ U^* = 50$) ($+$), $\Pi_1 = 500$ ($m^* = 220,\ U^* = 60$) ($\blacklozenge$) and $\Pi_1 = 1000$ ($m^* = 400,\ U^* = 40$) ($\triangle$).

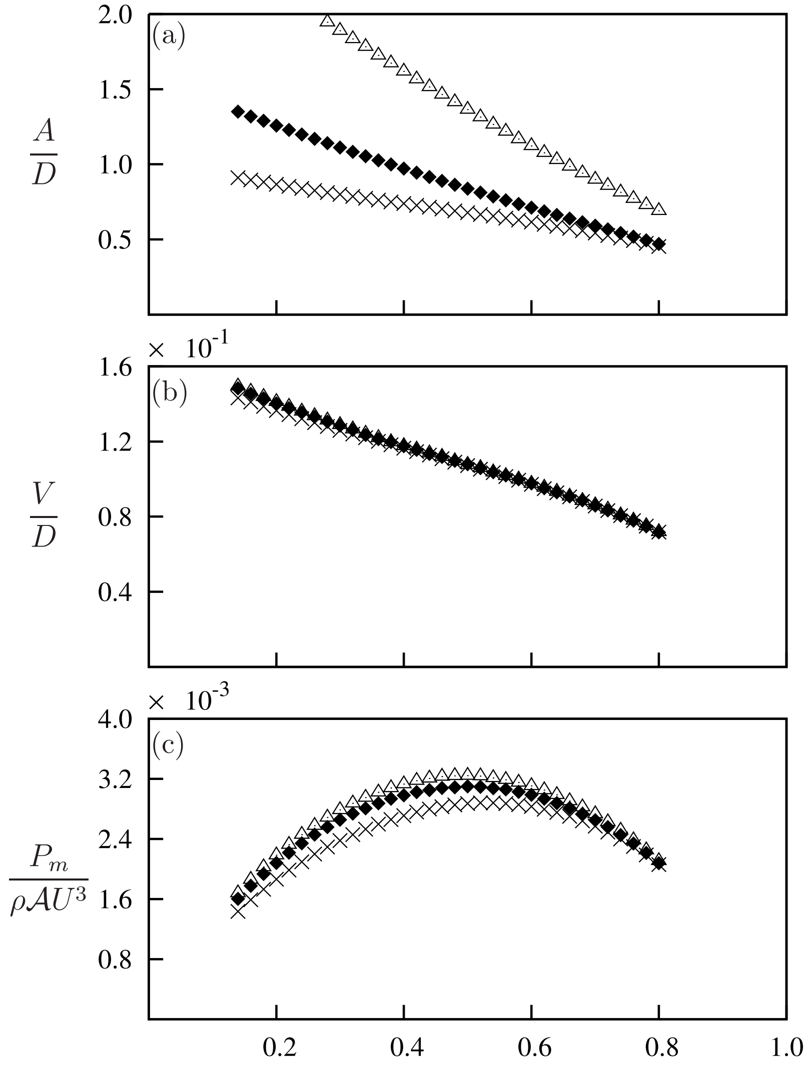

Figure 3: QSS data at high and low Π_1. (a) displacement amplitude, (b) velocity amplitude and (c) mean power as a function of Π_2. Data presented at $\Pi_1 = 10$ ($\times$), $\Pi_1 = 0.1$ (◆), and $\Pi_1 = 0.05$ ($\triangle$).

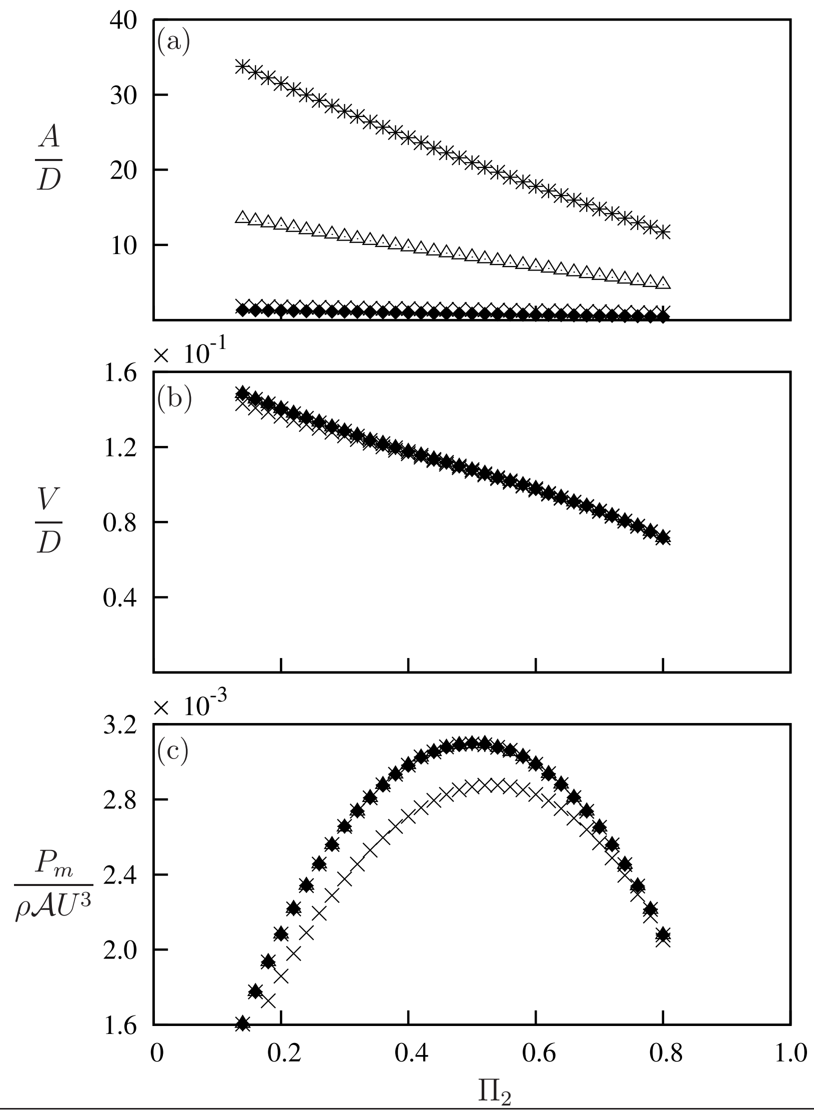

Figure 4: Comparison of QSS data at high and low Π_1. (a) displacement amplitude, (b) velocity amplitude and (c) mean power as a function of Π_2. Data presented at $\Pi_1 = 100$ ($\times$) $m^* = 130(+)$, $\Pi_1 = 0.1$ $m^* = 2$ (◆), $\Pi_1 = 0.1$ $m^* = 20$ ($\triangle$) and $\Pi_1 = 0.1$ $m^* = 50$ ($*$). The mass ratio does not have an effect on $\Pi_1$even at low Π_1

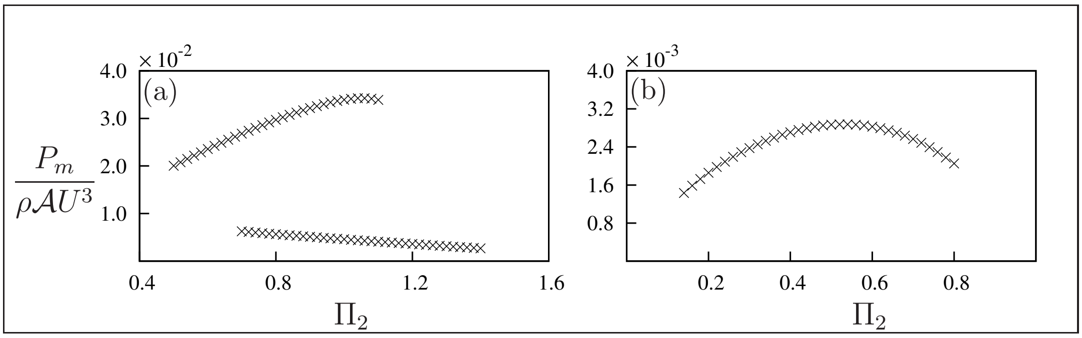

Figure 5: Mean power as a function of Π_2. Data presented at (a) $Re = 22300$, $\Pi_2 = 20000$ and (b) $Re = 200$, $\Pi_2 = 100$. Hysteresis could be observed at high Re

Π_1	% error
10	30.19%
60	10.71%
250	5.48%
1000	1.16%

Table 1: Error values of power between QSS and DNS data calculated using equation **??** at different $\Pi_1$and Π_2. data obtained at $U^* = 40$ and $Re = 200$

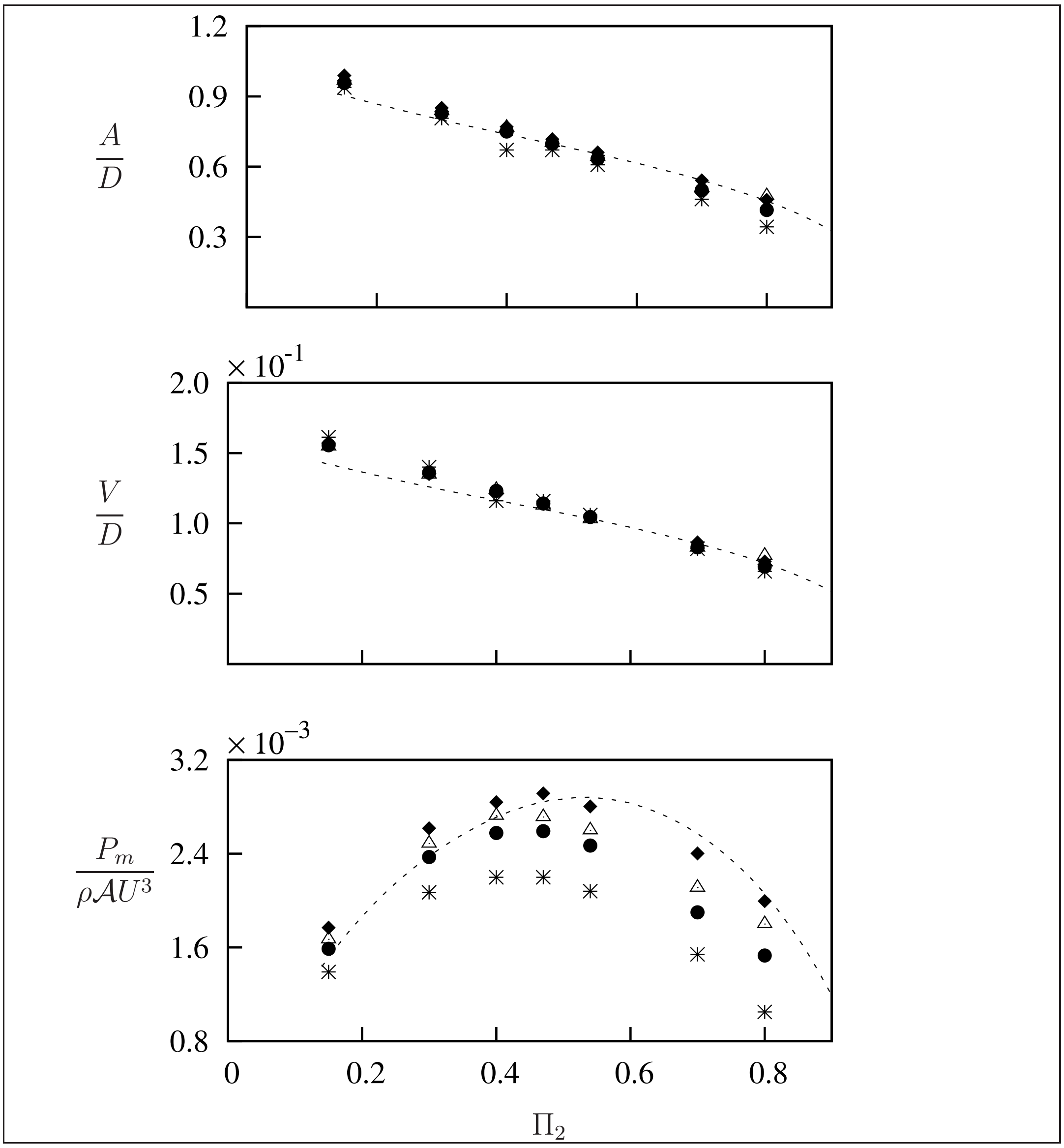

Figure 6: Comparison of data generated using the quasi-static theory and full DNS simulations . (a) Displacement amplitude, (b) velocity amplitude and (c) mean power as functions of Π_2. Data were obtained at Re = 200 at three different combined values $\Pi_1 = 10$ ($m^* \approx 20$) (✳), $\Pi_1 = 60$ ($m^* \approx 50$) (●), $\Pi_2 = 250$ ($m^* \approx 100$) (△), $\Pi_1 = 1000$ ($m^* \approx 250$) and $\Pi_1 = 6200$ ($m^* \approx 500$). The QSS data at $\Pi_1 = 10$ are represented by (- - -)

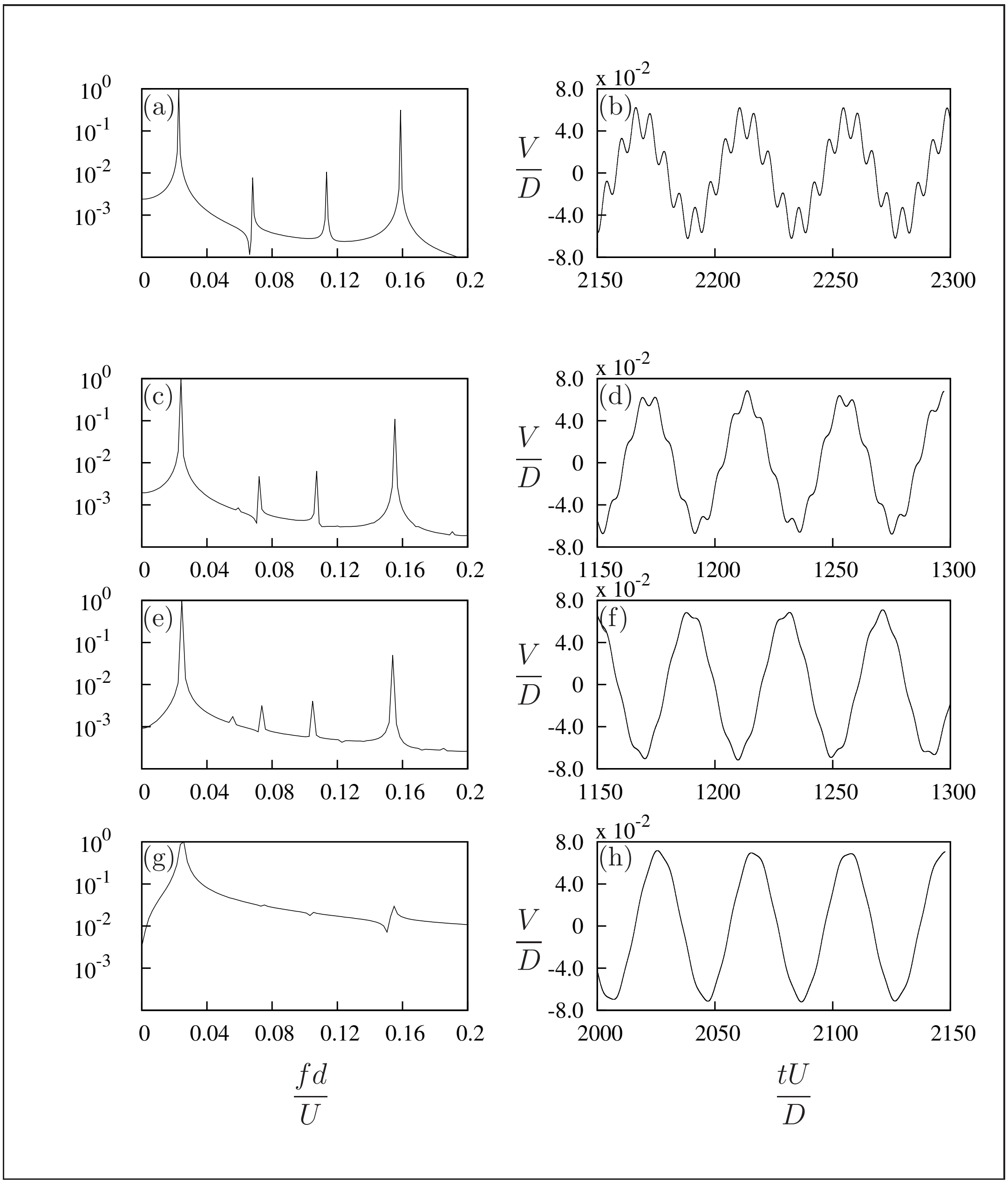

Figure 7: Velocity signal (right) and the corresponding power spectrum (left) of the DNS data at 3 different Π_1 at $\Pi_2 = 0.8$. (a) and (b) $\Pi_1 = 10$, (c) and (d) $\Pi_1 = 60$, (e) and (f) $\Pi_1 = 250$, (g) and (h) $\Pi_1 = 1000$. U^* is kept at 40 therefore the mass ratio increases ans Π_1 increases. It is evident that the influence of vortex shedding reduces as the inertia of the system increases.

References

Barrero-Gil, A., Alonso, G., Sanz-Andres, A., Jul. 2010. Energy harvesting from transverse galloping. Journal of Sound and Vibration 329 (14), 2873–2883.

Barrero-Gil, A., Sanz-Andrés, A., Roura, M., Oct. 2009. Transverse galloping at low Reynolds numbers. Journal of Fluids and Structures 25 (7), 1236–1242.

Den Hartog, J. P., 1956. Mechanical Vibrations. Dover Books on Engineering. Dover Publications.

Glauert, H., 1919. The rotation of an aerofoil about a fixed axis. Tech. rep., Advisory Committee on Aeronautics R and M 595. HMSO, London.

Griffith, M. D., Leontini, J. S., Thompson, M. C., Hourigan, K., 2011. Vortex shedding and three-dimensional behaviour of flow past a cylinder confined in a channel. Journal of Fluids and Structures 27 (5-6), 855–860.

Joly, A., Etienne, S., Pelletier, D., Jan. 2012. Galloping of square cylinders in cross-flow at low Reynolds numbers. Journal of Fluids and Structures 28, 232–243.

Leontini, J. S., Lo Jacono, D., Thompson, M. C., Nov. 2011. A numerical study of an inline oscillating cylinder in a free stream. Journal of Fluid Mechanics 688, 551–568.

Leontini, J. S., Thompson, M. C., 2013. Vortex-induced vibrations of a diamond cross-section: Sensitivity to corner sharpness. Journal of Fluids and Structures 39, 371–390.

Leontini, J. S., Thompson, M. C., Hourigan, K., Apr. 2007. Three-dimensional transition in the wake of a transversely oscillating cylinder. Journal of Fluid Mechanics 577, 79.

Luo, S., Chew, Y., Ng, Y., Aug. 2003. Hysteresis phenomenon in the galloping oscillation of a square cylinder. Journal of Fluids and Structures 18 (1), 103–118.

Ng, Y., Luo, S., Chew, Y., Jan. 2005. On using high-order polynomial curve fits in the quasi-steady theory for square-cylinder galloping. Journal of Fluids and Structures 20 (1), 141–146.

Païdoussis, M., Price, S., de Langre, E., 2010. Fluid-Structure Interactions : Cross-Flow-Induced Instabilities. Cambridge University Press.

Parkinson, G. V., Smith, J. D., 1964. The square prism as an aeroelastic non-linear oscillator. The Quarterly Journal of Mechanics and Applied Mathematics 17 (2), 225–239.

Thompson, M., Hourigan, K., Sheridan, J., Feb. 1996. Three-dimensional instabilities in the wake of a circular cylinder. Experimental Thermal and Fluid Science 12 (2), 190–196.

Thompson, M. C., Hourigan, K., Cheung, A., Leweke, T., Nov. 2006. Hydrodynamics of a particle impact on a wall. Applied Mathematical Modelling 30 (11), 1356–1369.

Vio, G., Dimitriadis, G., Cooper, J., Oct. 2007. Bifurcation analysis and limit cycle oscillation amplitude prediction methods applied to the aeroelastic galloping problem. Journal of Fluids and Structures 23 (7), 983–1011.